

Preparation and Characterization of Solid Dispersion of Tinidazole with Benzoic Acid and Tartaric Acid

Paola Vargas Escobar*, Oscar Albeiro Florez Acosta, Ana Liliana Giraldo Aguirre, Gloria Elena Tobón Zapata

Universidad de Antioquía
Colombia

*Corresponding author's email: [paola.vargase \[AT\] gmail.com](mailto:paola.vargase[at]gmail.com)

ABSTRACT—Two solid dispersions (SDs) were prepared in order to increase the dissolution rate of tinidazole (TND) by applying the method of grinding and moisturizing with drops of ethanol, using tartaric acid (TTA) and benzoic acid (BZA) as carrier agents. These carrier agents showed complete miscibility with TND, according to the DSC results. The two SDs were characterized and compared with pure TND through XRPD, DSC, FT-IR, particle size, water saturation solubility, equivalent specific surface, wettability and intrinsic dissolution rate tests. All samples were evaluated in the same particle range, and it was found that the increase in the dissolution of the two SDs in comparison to the pure drug was not a result of the reduced particle size but of the partial amorphization of the TND. The carrier-drug ratio makes the TND dosage in these two dispersions a promising alternative for the tablet form.

Keywords—Solid dispersion, tinidazole, saturation aqueous solubility, humectability, intrinsic dissolution rate

1. INTRODUCTION

The purpose of preparing the SDs is to enhance or improve the physicochemical properties of the active pharmaceutical ingredient (API). The properties depend on the characteristics of the molecule itself and how it is organized in the solid state, e.g. the dissolution rate, the hygroscopicity and the fluidity [1, 2,3]. SDs can be constructed by assembling a molecule of a drug and a carrier matrix that is composed of one or more pharmaceutically acceptable solids [4,5].

One particular characteristic of dispersed multicomponent systems is that the molecules are assembled by unions of non-covalent bonding forces, forming a single phase (miscible), and they can be prepared by means of various techniques, such as dry milling, milling with added solvent, solvent reduction, co-precipitation, fusion process, spray drying, freeze drying, supercritical fluid techniques, the use of intermediate stages, and other approaches [6]. If in the final assembly of these systems the product shows amorphous molecules in the system, it can be classified as a solid molecular dispersion [7-9].

Tinidazole (I - [2 - (ethylsulphonyl) ethyl]-2-methyl-5-nitroimidazole -TND) is an API actively distributed in some developing and European countries, and it is used as an antiprotozoal, antiamebic and antimicrobial agent, and it is also used to treat skin diseases [10]. With regard to its solubility, TND shows good dissolution in acetone, acetic anhydride and methylene chloride, but it is poorly soluble in both methanol and ethanol, and its solubility is low in both water and diethyl ether [11].

Therefore, it is a challenge to develop methods to increase the aqueous solubility and dissolution as a main characteristic of the TND. In previous reports, it has been shown that TND dissolution was improved by preparing co-crystals through the solvent evaporation technique, with lactose as a conformer, and in solid dispersions with polyethylene glycol (PEG 4000), hydroxypropyl methyl cellulose (HPMC 5cps), and β -cyclodextrin [12,13]. It has also been evidenced in previous reports that the use of microcrystals enhances the solubility [14]. The dispersions developed over the course of this research have not been mentioned in previous papers.

In this study, the solvent-drop grinding technique was used to prepare SDs for the purpose of improving the aqueous solution of TND using carboxylic acids (CAs) as pharmaceutical carriers. A subsequent physicochemical characterization was performed to the SDs that were obtained. This process allowed determining the properties and the mechanism

through which solubility is increased in relation to the pure drug. In said process, it was specifically observed if the decrease in the particle size of the product that resulted from the grinding was the determining factor.

Several different approximations were used in the characterization tests. These approximations were derived from the size of the solids and were easy to interpret with regard to the dissolution: the equivalent specific surface (ESS) was measured (due to the fact that the depth and density of the pores is a function of the particle size and the specific surface area of the solids), as well as the wettability measured in tablets, because it generally depends not only on the crystallinity, but also on the size of the compacted particles [15, 16]. Additionally, the study was aimed at obtaining systems with the minimum quantity of the carrier agent so that it would be practical for being dosed in the form of tablets, which is critical for TND due to the high quantity of the active ingredient generally contained in these dosage forms.

2. MATERIALES Y MÉTODOS

2.1 Materials

The 99.5% pure TND substance, the benzoic acid and the (+)-tartaric acid were used as received. Solvents were of analytical-reagent grade, and they were used without being purified. TND has a molecular weight of 247,273 g/mol, and it presented a melting point of 127-128 °C; while the molecular weight and melting point of the CAs were 150.08 g/mol and 171-174 °C for the L - (+) - tartaric acid, and 122.12 g/mol and 121-123 °C for benzoic acid.

2.2 Obtaining SD

Binary mixtures were prepared with different proportions (w/w) of TND/CA (1/3, 1/2, 1/1, 2/1, 3/1) by means of the technique of wetting the solid samples with drops of absolute ethanol while grinding them for 5 minutes. A porcelain mortar and a pestle were used to obtain a fine and dry powder. Instrumental comparisons were made between the simple physical mixtures (SMs) and the dispersions, and also with regard to the pure raw materials of both the TND and the CAs.

2.3 Evaluation and characterization of the SDs

Thermal analyses

Approximately 5 mg of the sample, which was previously dried at 105 °C for 1 hour, were used. DSC thermograms were obtained using a DSC Netzsch Fox-200 under a nitrogen atmosphere at 10 °C/min and open Al crucibles.

Infrared spectroscopy

The analyses were conducted on an FT-IR Perkin Elmer Spectrum BX, in which the samples were diluted in KBr tablets, and the reading was made between 4000 and 600 cm⁻¹.

Powder X-Ray Diffraction (PXRD)

Measurements were performed on a PANalyticalEmpyrean diffractometer, using CuK_{α1} radiation over the 2θ region and scanning from 5° to 40°.

2.4 Characterization tests performed to the obtained SDs and the pure drug

Particle size

The distribution frequency of the mean equivalent volume diameter of surface of the particles (d_{vs}) was calculated using an optical light microscope BOECO BM-180 T/SP, which was adapted to a Microsoft Lifecam Vx-6000 digital camera. The thin films produced through the grinding process and the pure solid TND were sieved to select samples retained between screens 230 (63 microns) and 325 (44 microns) of Tyler sieves (ASTM E11, 2009) in such a way that the size range of the solid samples was similar.

True density (ρ)

A helium pycnometer (Accupyc II 1330, Micromeritics, USA ®) was used for measuring the volume of accurately weighed one-gram samples.

Equivalent specific surface (ESS)

The surface of the samples was calculated by approximating it to the shape of a sphere and using the values of density and diameter, as it is shown in Equation 1 [17, 18].

$$ESS = \frac{6}{\rho d_{vs}} \quad (\text{Equation 1})$$

Determination of water saturation solubility

The tests were performed in triplicate for both the pure drug and the obtained SDs. An excess of the solid samples was used in eight phosphate buffers with different pH values: 1.48, 3.05, 4.76, 6.10, 7.18, 8.10, 9.30, and 11.55. The tubes were left under constant stirring for 5 days at a temperature of 37 °C. Then, the solutions were filtered and the TND concentration was determined in a Hasch DR 5000 UV-vis spectrophotometer at 317 nm, using a calibration curve and sodium benzoate as hydrotropic agent [19].

2.5 Tablets for the assays

The tablets were made with a locally-built, calibrated monopunzon hydraulic press (Model 060804 Compac, IndemecLtda, Itagüí-Colombia), using flat-faced punches (with a diameter of 11.5 mm).

Surface energy of the solid tablets (σ_s)

The calculation was based on the wettability measurement results. For such purpose, the sessile drop method was used in a closed chamber at 37 °C, depositing 3-6 μ l of milli-Q water on SDs and TND tablets. The contact angle (θ) between the water droplet and the tablets was evaluated on the digital image. The analysis was performed with the ImageJ software, using the *Contact Angle* plugin [20]. Subsequently, Equation 2 (as proposed by Young) was used to obtain the surface energy of the solid samples.

$$\sigma_s = \sigma l + \sigma \cos \theta \quad (\text{Equation 2})$$

Where σ_s is the surface tension or wettability of the solids with respect to the water, in this case. The l value for the water (σl) at 37 °C was 71.00 mN/m. The determination of σ_s was based on Neumann's theory, in which $\sigma l = f(\sigma, \sigma_s)$, as well as Berthelot's approximation, according to Equation 3 [21]:

$$\sigma l = \sigma + \sigma_s - 2\sqrt{\sigma \cdot \sigma_s} \quad (\text{Equation 3})$$

Equation 4 was obtained by substituting Equation 3 into Equation 2:

$$\sigma_s = \frac{\sigma(1 + \cos \theta)^2}{4} \quad (\text{Equation 4})$$

2.6. Intrinsic dissolution test (IDR)

The test was performed six times with both the TND as the two SDs by using the stationary disk system. The samples were pressed at 7 MPa for 30 s directly into stainless steel discs that have a sealed cavity and a diameter of 11.5 mm (1.039 cm²). The discs were placed at the bottom of dissolution vessels containing 900 ml of deionized and degassed water. The glasses were placed into an Erweka DT6 series dissolutor, and the content was stirred with type 2 paddles at 100 rpm and at a temperature of 37 °C [22]. The concentration readings were done in appropriate intervals, taking 5 ml of the solution in order to read the aliquots in the UV-visible spectrophotometer at a λ of 317 nm.

Based on Equation 5, the IDR was obtained from the slope of the linear regression, where the accumulated amount dissolved in time was evaluated in relation to the surface area. Only the first portion of the graph, the part with linear behavior, was considered.

$$IDR = \left(\frac{dw}{dt} \right) \left(\frac{1}{S} \right) \quad (\text{Equation 5})$$

Where IDR is measured in mg/min/cm², dw/dt is the amount of mg of TDN dissolved per unit of time (min), and S is the area (cm²) [23].

3. RESULTS AND DISCUSSION

3.1 Obtaining SD

The solvent-drop grinding technique was used to obtain, through DSC analysis, a sharp endothermic melting signal lower than the signals of the pure substances (mp), as shown in Figure 1. The carrier load of tinidazole/tartaric acid (TND/TTA) and tinidazole/benzoic acid (TND/BZA) is within the limits of the eutectic composition of the binary systems, which allows obtaining the proportions of 2:1 (w/w), and it has a simple phase with visible differences between the SDs and the SMs.

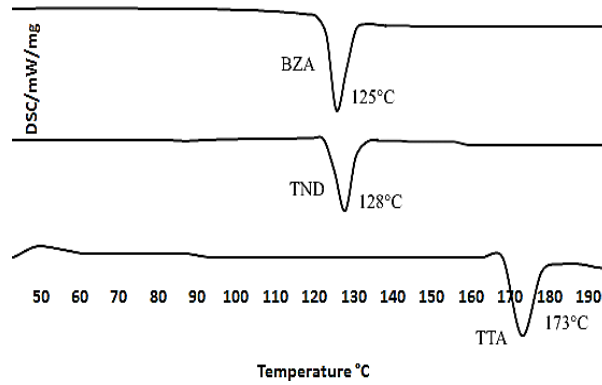


Figure 1. DSC curves with melting points for the pure raw materials.

The thermograms of the dispersions and the simple mixtures are shown in Figure 2, where the decrease in the fusion signals reveals the increased miscibility and reduced crystallinity of the TND in the dispersions. These observations are the opposite of the observations made in the solid physical mixtures, which presented the two melting endothermic fusion signals of the respective CAs, the drug and of the physical interaction between them.

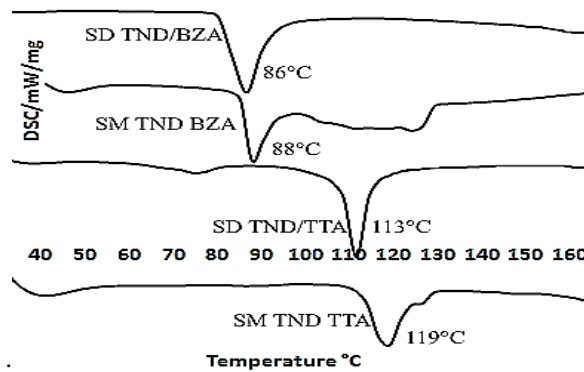


Figure 2. DSC curves with the melting points of the two obtained dispersions and the corresponding simple mixtures

Similarly than in the thermograms, the results of the PXRD patterns of the pure drug and the organic acids are presented in Figure 3, showing the three characteristic crystalline solids.

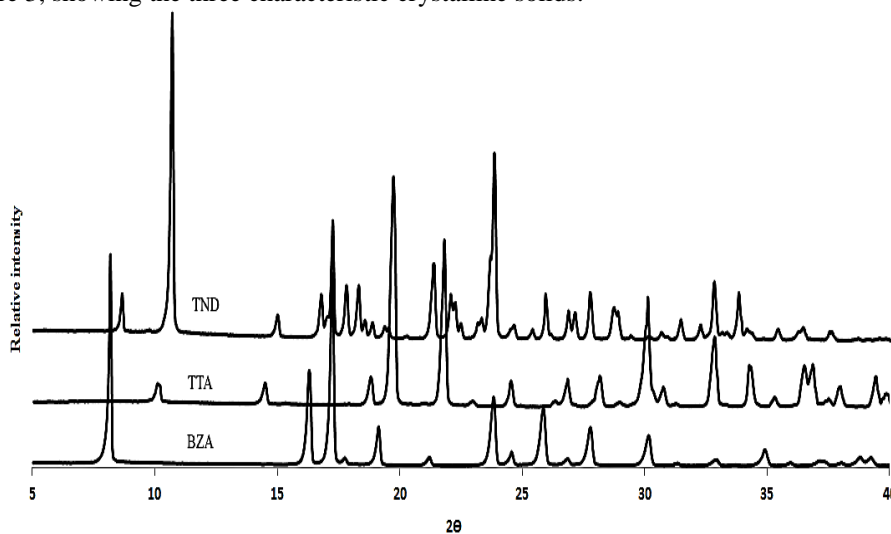


Figure 3. PXRD patterns of pure original substances.

Consecutively, the relative intensity of the main individual signals was calculated in relation to the greatest peak based on the PXRD signals shown in Figure 4. The calculation (not shown here) evidenced differences between the

dispersions and the physical blends of the same composition, confirming the amorphization of the drug in the dispersion with each of the carriers.

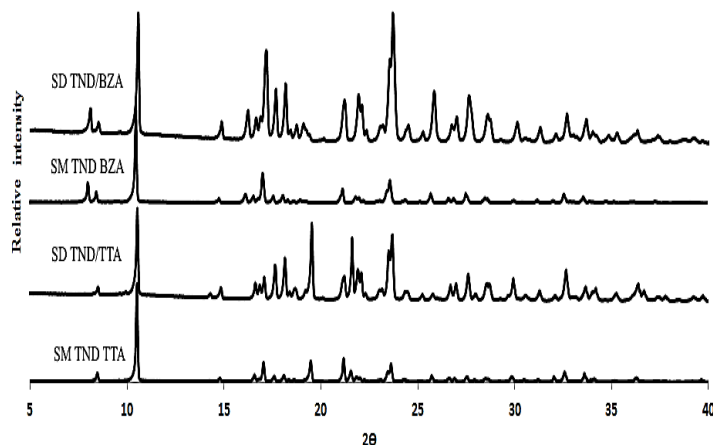


Figure 4. PXRD patterns of the dispersions and the solid physical mixtures.

In the FT-IR spectra shown in Figure 5, the characteristic signals of the combination of the original raw materials were found with some differences between the SMs and the obtained SDs.

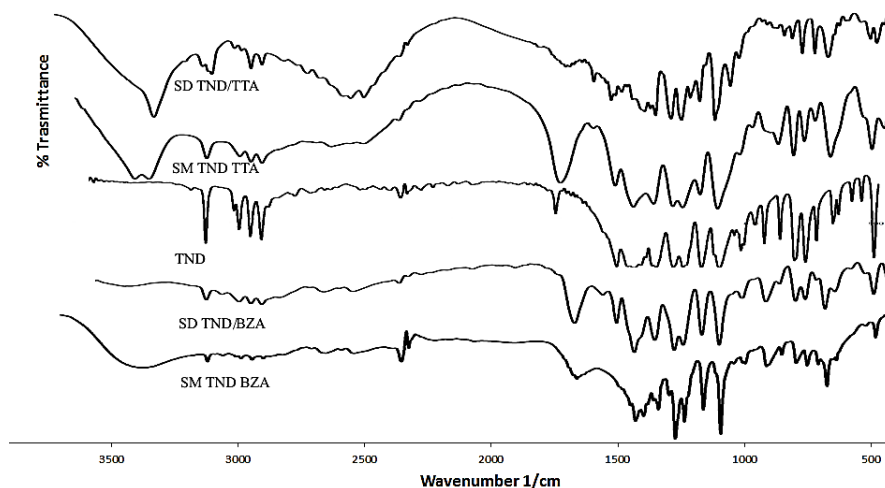


Figure 5. Comparison of FTIR spectra of the dispersions and the solid physical mixtures.

The infrared spectrum of the TND showed the following main absorption peaks: at 3130 cm^{-1} , typical of the N-H stretch, supplemented with the signal at 943 cm^{-1} by the stretching vibration of C-N; at 3000 cm^{-1} and 2910 cm^{-1} , it showed asymmetric and symmetric vibrations of the aromatic CH; at 2960 cm^{-1} it showed a peak due to the stretching vibration of CH; at 1750 cm^{-1} , it showed a peak of C=O; at 1536 cm^{-1} , it presented asymmetric vibrations due to the NO_2 , and the vibrations were symmetrical at 1368 cm^{-1} ; at 1456 cm^{-1} , it presented an aromatic C=C stretching vibration; and at 1040 cm^{-1} , it showed the vibration plane corresponding to the CH bending imidazolium ring.

However, most of these peaks changed or disappeared in both solid dispersions: almost all signals decreased in TND/BZA, except for the signals at 1450 and 945 cm^{-1} . In the case of the TND/TTA dispersion, the signals corresponding to the drug decreased or disappeared, as it was the case for the peaks at 1536 cm^{-1} and 945 cm^{-1} . The spectra of the simple mixtures of TND with BZA and TTA were presented as overlays of the individual spectra of the raw materials.

3.2 Evaluation and characterization of the obtained dispersions

As it can be observed in Figure 6, there are differences between the maximum water saturation solubility of TND as pure drug and the dispersions. TND/BZA showed the highest solubility at $37\text{ }^\circ\text{C}$ (45.0 mg/ml), followed by TND/TTA (30.2 mg/ml) and, finally, TND (21.7 mg/ml).

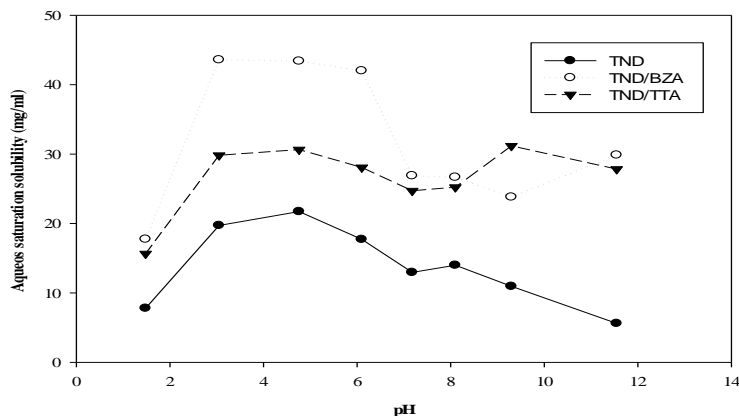


Figure 6. Graph of water saturation solubility vs. pH of both SDs and the pure drug.

Other features of the two SDs related to pure TND are presented in Table 2. In the texture characterization of the tablets, two interrelated aspects were evaluated: the specific surface of the solid (ESS) and the density. The results showed a higher ESS in the TND/BZA dispersion, and a very similar ESS between the TND/TTA and the pure drug, while the density was lower for the TND than for the dispersions. This last result could be opposite to the best dissolution, but the wettability of a solid not only depends on the surface the solvent can access, but also on the surface energy of the solid.

Based on the information of the foregoing paragraph, the intermolecular forces of the surface of the tablets were measured, evaluating them as surface energy in comparison to the water and based on the contact angle $-\theta^\circ$ (shown in Table 1). Then, the surface energy parameter (σ_s) was obtained for each one of the surfaces of the compressed solid samples, finding higher σ_s values for the two SDs than for the pure drug. This last observation could be evidence of the best dissolution of the dispersions.

Table 1. Properties of both the pure drug in solid state and the dispersions: mean volume-surface diameter of the particles (*dvs*); true density (ρ), equivalent specific surface (ESS), contact angle (θ°), and surface energy (σ_s). The values in parentheses correspond to the standard deviation.

	<i>Dvs</i> (μm)	ρ (g/cc)	ESS ($10^{-3} \text{ m}^2/\text{g}$)	θ ($^\circ$)	σ_s (J/m^2)
TND/BZA	153.22 (1.55)	1.639 (0.02)	238.93 (17.01)	56.21	42.38 (3.01)
TND/TTA	237.78 (1.84)	1.666 (0.01)	151.45 (10.24)	60.43	39.03 (2.64)
TND	109.46 (1.65)	1.466 (0.02)	373.93 (35.52)	76.73	26.45 (2.51)

*The values in parentheses correspond to the standard deviation.

The IDR test was assessed using the linear regression of the data at 0, 10, 15 and 30 minutes for tablets of the two SDs and for the TND. The dissolution profiles of Table 2 show that the two systems had similar results and a faster release of the active agent in comparison to the pure drug. The test results are shown in Figure 7, from which the following IDR values were obtained in $\text{mg}\cdot\text{min}^{-1}\cdot\text{cm}^{-2}$ units: 0.65 for TND/BZA, 0.57 for TND/TTA, and 0.30 for TND. This analysis confirms that the IDR is not dependent on the particle size because the surface area is almost constant over time and the dissolution rate depends primarily on the characteristics of the solute, hydrodynamic and diffusion coefficient in the dissolution medium [23].

Table 2. Amount (mg) dissolved per time unit for the dispersions and the pure drug, with the corresponding standard deviation presented in brackets.

Time (min)	TND/BZA (mg)	TND (mg)	TND/TTA (mg)
10	7.37 (0.40)	3.48 (0.46)	7.06 (0.88)
15	10.13 (0.77)	4.82 (0.15)	9.49 (0.79)
30	20.48 (2.17)	9.37 (1.04)	18.01 (1.52)

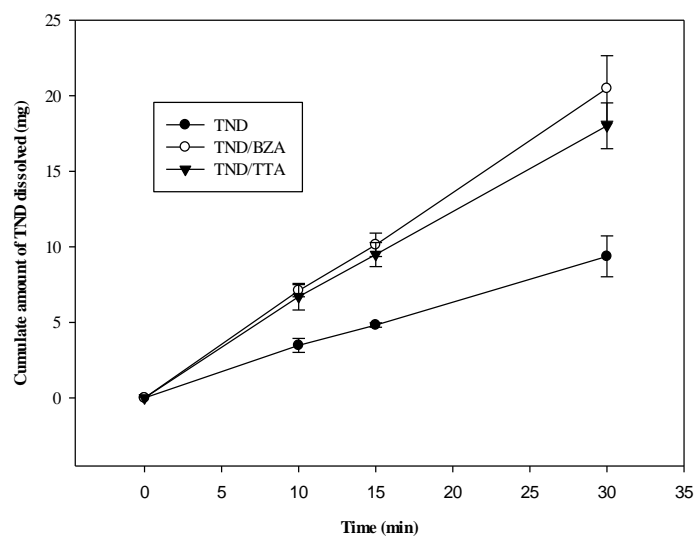


Figure 7. Plot of the intrinsic dissolution rate (IDR) in water

The obtained multicomponent systems showed complete miscibility but did not establish new bonds, revealing the formation of two solid dispersions instead of other systems. Considering that the three species were evaluated in the same particle size range, the mechanism that would most likely increase the dissolution of these dispersions with regard to the pure drug is the increased amorphization of the component substances, additionally to an active micro-environment produced by the CAs around the molecules of the active principle, which facilitates the solubilization process.

4. CONCLUSIONS

This study allowed establishing that the two SDs prepared by means of the wet milling technique improve the solubility and the TND dissolution rate in comparison to the pure drug when it is modified as solid dispersions using two CAs as conformers. The obtained SDs, TND/BZA and TND/TTA, showed very similar responses among themselves in both the characterization and dissolution tests, but they presented different responses to the pure drug. No relationship was found between the particle size of the SDs and the dissolution rate. Finally, it should be noted that the two obtained dispersions are prepared with a higher proportion of the drug than the one for the carrier, differently to most non-covalent multicomponent systems, which represents an advantage for the preparation of tablets as a pharmaceutical dosage form.

5. ACKNOWLEDMENT

The authors are especially grateful to the Faculty of Pharmaceutical and Food Sciences of the University of Antioquia for their continued support and for providing the necessary resources for this research.

6. REFERENCES

- [1] Yanbin Huang, Wei-Guo Dai. Fundamental aspects of solid dispersion technology for poorly soluble drugs. Review. *Acta Pharmaceutica Sinica B*;4(1):18–25, 2014.
- [2] Chau Le-Ngoc Vo, Chulhun Park, Beom-Jin Lee. Current trends and future perspectives of solid dispersions containing poorly water-soluble drugs. *European Journal of Pharmaceutics and Biopharmaceutics* 85: 799–813, 2013.
- [3] Yanbin Huang, Wei-Guo Dai. Fundamental aspects of solid dispersion technology for poorly soluble drugs. *Acta Pharmaceutica Sinica B*;4(1):18–25, 2014.
- [4] Dumbre K.A, Gadhave M.V, Gaikwad D.D. Development, evaluation and characterization of surface solid dispersion for solubility and dissolution enhancement of nifedipine. *Asian Journal of Pharmaceutical Research and Development* Vol. 2 (3) May–June 70-77, 2014.
- [5] Iswarya Sridhar, Abha Doshi, Bhagyashri Joshi, Vandana Wankhede, Jesal Doshi. Solid Dispersions: an Approach to Enhance Solubility of poorly Water Soluble Drug. *Journal of Scientific and Innovative Research* 2 (3): 685-694, 2013.
- [6] Rodríguez-Spong B , Price CP , Jayasankar A , Matzger AJ , Rodríguez-Hornedo Nr. General principles of pharmaceutical solid polymorphism: A supramolecular perspective. *Advanced Drug Delivery Reviews*. 56(3):241-74, 2004.
- [7] Vishweshwar P, McMahon JA, Bis JA, Zaworotko MJ. Pharmaceutical co-crystals. *Journal of Pharmaceutical Sciences* 95(3):499-516, 2006.
- [8] Stahly GP. A Survey of Cocrystals Reported Prior to 2000. *Crystal Growth & Design* 9(10):4212-29, 2009.
- [9] Manes G, Balzano A. Tinidazole: from protozoa to *Helicobacter pylori*--the past, present and future of a nitroimidazole with peculiarities. *Expert Rev Anti Infect Ther*. 2004 Oct; 2(5):695-705
- [10] EP. *European Pharmacopoeia*. 5 ed 2004. Council of Europe, V2. pg 2585. 2727, 2004.
- [11] Paun Jalpa S., Chapla Vishal K., Raval Mihir K., Tank Hemraj M Improvement of Physicochemical properties of tinidazole cocrystals: An Influence Of Additives. *Indo American Journal of Pharm Research*,3(5). p3680-3688, 2013.
- [12] Puckhraj Chhaprel, Amit Talesara, Amit K Jain. Solubility enhancement of poorly water soluble drug using spray drying technique. *International Journal of Pharmaceutical Studies and Research*, 3(2):01-5, 2012.
- [13] P. Sabitha Reddy, S. Sujani and K. Ravindra Reddy. Microcrystals: For Improvement of Solubility and Dissolution of Tinidazole. *Asian J. Pharm. Tech*, Vol. 1: Issue 3, Pg 64-69, 2011.
- [14] Agarwal V. Dissolution and powder flow characterization of solid self-emulsified drug delivery system (SEDDS). *International Journal of Pharmaceutics* 366, 44–5 , 2009.
- [15] Paun J. CV, Raval M., Tank H M. Improvement Of Physicochemical Properties Of Tinidazole Cocrystals: An Influence Of Additives. *Indo American Journal of Pharmaceutical Research*, 3(5):3680, 2013.
- [16] Stamboliadis ET. The energy distribution theory of comminution specific surface energy, mill efficiency and distribution mode. *Minerals Engineering*, 20(2):140-5, 2007.
- [17] Wells JI. *Pharmaceutical preformulation: the physicochemical properties of drug substances*. 227 p, United Kingdom, 1988.
- [18] Maheshwari R, Chaturvedi S, Jain N. Novel spectrophotometric estimation of some poorly water soluble drugs using hydrotropic solubilizing agents, march 1, 2006. 195-8 p, 2006.
- [19] National Institutes of Health. ImageJ, Bethesda, Maryland, USA, [revised 2014 November 26; cited 2016 February 26]. Available from: <http://rsbweb.nih.gov/ij/>;
- [20] Kwok DY, Neumann AW. Contact angle interpretation in terms of solid surface tension. *Colloids and Surfaces A: Physicochemical and Engineering Aspects*, 161(1):31-48, 2000.
- [21] Joshi SS, Hilegaonkar SB. Verification of official Dissolution Media for Tinidazole. *Journal of Pharmacy Research*, 3(7), 2010.
- [22] Zakeri-Milani P, Barzegar-Jalali M, Azimi M, Valizadeh H. Biopharmaceutical classification of drugs using intrinsic dissolution rate (IDR) and rat intestinal permeability. *European Journal of Pharmaceutics and Biopharmaceutics*;73(1):102, 2009.
- [23] Hendriksen BA, Williams JD. Characterization of calcium fenoprofen 2. Dissolution from formulated tablets and compressed rotating discs. *International Journal of Pharmaceutics*, 69(2):175-80, 1991.